# Angular Momentum of Electromagnetic Field in Areas of Polarization Singularities

Mokhun I., Brandel R. and Viktorovskaya Ju.

Chernivtsy University, 2 Kotsyubinsky St., Chernivtsy, 58012 Ukraine
mokhun@itf.cv.ukrtel.net

Received:02.03.2006

## Abstract

It is shown that physical manifestations of any optical singularity are, in one way or another, related to a specific temporal behaviour of the field, no matter scalar or vector cases are realized. Polarization singularities of the vector field are associated with a presence or absence of angular momentum of electromagnetic field. In the vicinity of $C$-point the orbital angular momentum is observed if the sings of topological charge of the vibration phase and the handedness factor are different.

**Keywords:** polarization singularities, Poynting vector, angular momentum.

**PACS:** 42.50.Ct

## 1. Introduction

It is known that optical singularities are divided into scalar and vector ones [1-20]. Scalar vortices (i.e., stationary intensity zeroes) represent principal singularities of scalar fields [1-8]. It has been noticed that, contrary to the scalar fields, stationary amplitude zero of vector field (at least, for the random fields) is nongeneric [3,9]. At the same time, stationary characteristics of the vector fields (e.g., the vibration phase or the parameters of polarization ellipses such as the polarization azimuth, the ellipticity and the rotation direction) may also possess singularities, which have been called as polarization singularities [3,10-20].

In the paraxial approximation, spatial distribution of polarization ellipses maintains polarization singularities of two kinds: $S$-surfaces and $C$-lines [3,10-15] (in the observation plane, we have $s$-contours and $C$-points, respectively – see Fig. 1). The field is linearly polarized on the $s$-contours and the direction of electric vector rotation is indeterminate. The $C$-points are points where the field is circularly polarized (as a consequence, the polarization azimuth and the vibration phase are then indefinite [3,9-15,17]). The $C$-points are characterized with the Poincar´e-Hopf index $I_C$ that describes orientations of the ellipsis axes in the surrounding planar vector field and the topological charge of the vibration phase $S_C$ [3,9-15].

Polarization singularities are peculiar sets of field. The field characteristics (like the polarization azimuth, the vibration phase and the rotation direction of the field vector) change as much as possible in their vicinity. Moreover, those characteristics suffer jump-like changes when crossing the singular set (see Fig. 1a). At the same time, the field points associated with the singularity and those localized near it are not distinguished within the common optical approaches (for example, in polarimetry). Indeed, the field behaviour is practically the same at the singularity point and its close area (the $A$ and $B$ areas in Fig. 1b). The modulus and temporal orientation of the field vector have

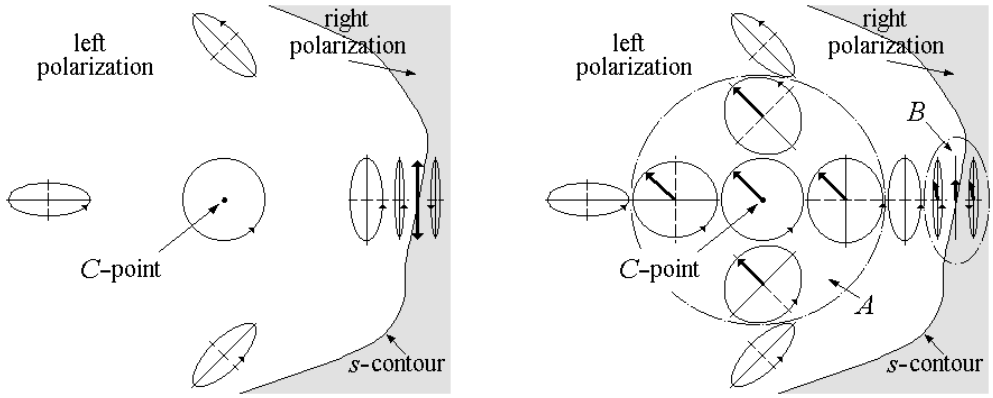


**Fig. 1.** Qualitative behaviour of vector field in the vicinities of $C$-point and $s$-contour. $A$ area is a vicinity of the $C$-point with practically the same behaviour of the field and $B$ area means a region with the polarization close to the linear one.

very small distinctions at the $C$-point and the points of the $A$ region. The polarization is practically linear inside the $B$ area.

It seems that the above considerations would lead to obvious conclusion: the only reason for studying optical singularities should consist in their role in formation of the structure of light fields, both scalar and vector. On the other hand, singularity of any field parameter unavoidably gives rise to some physical peculiarities of the field in its vicinity. Then the question arises: which are physical manifestations of the optical singularities characterized by specific behaviour of physical system affected by electromagnetic wave?

It is obvious that similar motivation concerning the physical manifestation of scalar vortices may be adduced. But the question answered above does not appear, because, as it is known, orbital angular momentum of the field arises in the vortex vicinity [21-33] and this fact clearly evidences physical "exclusiveness" of field structure with the vortex. Orbital angular momentum appears due to a specific helicoidal shape of phase surface in the vortex area, and so it is a result of a specific temporal behaviour of this field. In this sense, vortex as a physical structure must be considered as a *temporal singularity*. As to polarization singularities, they *also must be considered as temporal ones*, in the end, because the singular parameters (the azimuth and the vibration phase) define the state of field vector not only in *space* but in *time*, too.

The answer about the temporal peculiarity of $s$-singularity is trivial and it follows immediately from the nature of the $s$-contour: spin angular momentum of any field vanishes in the vicinity of this line owing to linear polarization of the field along it. The temporal peculiarity in the $C$-point area is not so obvious as in the $s$-set case. We are stating here that such the peculiarity is connected with the other kind of angular momentum, namely the orbital one. It is known [34,35] that the phenomenon takes place in some specific cases, e.g., for the conical diffraction [36]. Nonetheless, the following question arises: does the appearance of orbital momentum always accompany formation of the field structure with the $C$-point? In this paper we attempt to substantiate such the point of view.

## 2. Angular momentum in the vicinity of optical singularities

Let us consider the Poynting vector (PV) in the paraxial approximation. In this connection, we will not average the corresponding magnitudes over the space coordinates and time, in contrast to the conventional approach [21-33]. Let us rather try to keep the space and temporal

dependences practically to the very end of the analysis.

First of all, we define the strengths of electric and magnetic fields as

$$\begin{cases} E_x = e_x \cos(\omega t + \Phi_x - \mathbf{kr}) \\ H_x = h_x \cos(\omega t + \tilde{\Phi}_x - \mathbf{kr}) \end{cases}, \quad (1)$$

and similarly for the $y$ and $z$ components. Here $e_x, h_x, \ldots$ and $\Phi_x, \tilde{\Phi}_x, \ldots$ are respectively the amplitude modules and the phases of the corresponding field components.

Except for the areas localized in immediate proximity to some specific field points (for example, the centres of vortices), **kr** may be replaced with $kz$ ($k = \frac{\omega}{c}$ being the wave number). Then Eq. (1) transforms to the form

$$\begin{cases} E_x = e_x \cos(\omega t + \Phi_x - kz) \\ H_x = h_x \cos(\omega t + \tilde{\Phi}_x - kz) \end{cases}, \quad (2)$$

etc. As it is known [10,22], the following equations are valid for the paraxial approximation and the wave propagating in vacuum:

$$-\frac{j}{k} rot\mathbf{U} = \mathbf{V}, \quad (3)$$

$$U_z^z \approx -jkU_z, \quad (4)$$

where **U** and **V** mean respectively the complex wave functions of the electric and magnetic fields and $U_z^z$ is derivative of $U_z$.

It can be shown that the relations for the PV components, which contain characteristics of the electric field alone, may be obtained by using Eqs. (3) and (4) and the PV definition. Note also that $E_x$ may be determined by the $E_x$ and $E_y$ components [22], due to Eq. (4). As a consequence, the following system defined only by characteristics of the $x$ and $y$ components of the electric field is valid, at least for the far field:

$$\begin{cases} P_x \approx -\frac{c}{4\pi k}\{E_x T_2 - E_y T_1\} \\ P_y \approx -\frac{c}{4\pi k}\{E_y T_2 + E_x T_1\}, \\ P_z \approx \frac{c}{4\pi}\{E_x^2 + E_y^2\} \end{cases} \quad (5)$$

where

$$\begin{cases} T_1 = E_x \Phi_x^y - E_y \Phi_y^x + \frac{e_x^y}{e_x} E_{x,\frac{\pi}{2}} - \frac{e_y^x}{e_y} E_{y,\frac{\pi}{2}} \\ T_2 = E_x \Phi_x^x + E_y \Phi_y^y + \frac{e_x^x}{e_x} E_{x,\frac{\pi}{2}} + \frac{e_y^y}{e_y} E_{y,\frac{\pi}{2}} \end{cases} \quad (6)$$

and

$$\begin{cases} E_i = e_i \cos(\omega t + \Phi_i - kz) \\ E_{i,\frac{\pi}{2}} = e_i \sin(\omega t + \Phi_i - kz) \end{cases}. \quad (7)$$

Here $e_i$ and $\Phi_i$ denote the modules of the amplitude and the phases of the components, respectively, $e_i^l, \Phi_i^l$ are their derivatives and $i, l = x, y$. Accordingly, we get

$$\left|\mathbf{P}_t\right| = \frac{1}{k}\{\frac{c}{4\pi} P_z (T_1^2 + T_2^2)\}^{1/2}, \quad (8)$$

where $\mathbf{P}_t$ is the transversal component of the PV.

Let us mark that inequality of $z$ component of the field to zero is a mandatory requirement for inequality of the transversal PV component to zero. Assume now that the wave of a general kind has a nonzero $z$ component, e.g., due to some curvature of the wave front and that the field rotates in the plane perpendicular to the $z$ axis. In this case the transversal component of the PV also rotates in the vicinity of some point in this plane. Rotation of the PV component corresponds to energy transport in the transversal direction. Obviously, an averaged angular momentum then appears, with the point of application located in the rotation centre. Generally, an averaged orbital angular momentum would appear due to any kind of the PV rotation, and this holds for the vector fields, too. One can state that there is absolutely no difference whether this rotation is a result of experimental tricks or a natural consequence of formation of specific temporal field structure. Only one distinction arises: the optician cannot "observe" energy rotation in the latter case, because of the fact that the rotation frequency is comparable to that of the light vibration.

Let us now return to Eq. (8). It can be easily seen that the module of the transversal PV component is defined by the longitudinal one. As a result, the transversal component of the PV rotates if the longitudinal one changes cyclically owing to specific temporal behaviour of the $x$ and $y$ field components. Let us test this statement on the example of scalar vortex. The intensity distribution in the vortex vicinity is presented in Fig. 2a. The relations for the Cartesian PV components in case of the isotropic vortex [6] polarized, e.g., in the $x$ direction may be written in the polar coordinates $\rho, \phi$ as

$$\begin{cases} P_t \sim e_x \left|\cos(\omega t + S\phi - kz)\right| \\ P_z \sim e_x^2 \cos^2(\omega t + S\phi - kz) \end{cases}, \qquad (9)$$

where $S$ is topological charge of the vortex.

Thus, the longitudinal component of the PV behaves specifically in the vortex vicinity. Its maximum (or minimum) rotates around the vortex centre with the frequency twice as much as that of the light vibration. The transversal component rotates, too (see Fig. 2b). The rotation direction is determined by the sign of topological charge of the vortex and the minimum of the energy density is located along the dark straight line. Such the minimum corresponds to instantaneous field zero and may be interpreted as "lengthy" Nye's disclination (see, e.g., [3, 9-11]).

## 3. Angular momentum in the area of $C$-point

Let us mention that the $C$-point appears in the position, where one of orthogonal circularly polarized components of the vector field has its exact stationary intensity zero [3,9-11,14,15]. Circularly polarized component vortex is formed in the $C$-point position. The simplest polarization cell with the $s$-contour and the $C$-point may be brought about as a superposition of two coaxially propagating, orthogonal circularly polarized beams. One of them represents a circularly polarized isotropic vortex and the second one is orthogonally polarized plane wave. Let us put the origin of the polar coordinate system to coincide with the vortex centre. The complex amplitudes of these superposing beams (in terms of orthogonal linearly polarized components) may be written in the following form:

$$\begin{cases} U_{Vx} = \rho \exp(jS\varphi) \\ U_{Vy} == \rho \exp[j(S\varphi + h\frac{\pi}{2})] \end{cases}, \qquad (10)$$

$$\begin{cases} U_{Rx} = 1 \\ U_{Ry} == \exp(-jh\frac{\pi}{2}) \end{cases}, \qquad (11)$$

where $\varphi$ and $\rho = \sqrt{x^2 + y^2}$ are the polar coordinates, $S$ the topological charge of the vortex and $h$ the handedness factor, which is equal to $+1$ or $-1$ respectively for the right or left polarizations. Then the $x$ and $y$ components of the resulting field are as follows:

$$\begin{cases} U_x = 1 + \rho\cos\varphi + jS\rho\sin\varphi \\ U_y = -jh + \rho\cos(S\varphi + h\frac{\pi}{2}) + \\ \qquad + j\rho\sin(S\varphi + h\frac{\pi}{2}) \end{cases}. \qquad (12)$$

After a little algebra involving Eqs. (5)–(7),

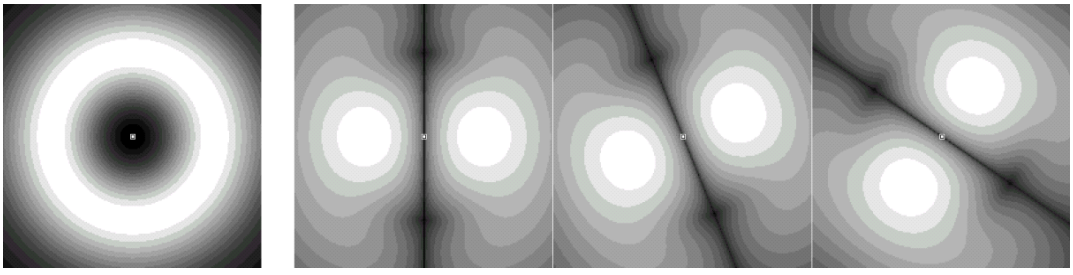

*a* *b*

**Fig. 2.** Temporal rotation of energy density around the vortex centre: (a) intensity distribution in the vortex vicinity, (b) temporal rotation of the transversal PV component.

one can prove that the instantaneous transversal components of the PV are given by

$$\begin{cases} P_x = -\dfrac{c}{4\pi k}\{\dfrac{1-Sh}{S-h}\times \\ \quad \times \sin[2(\omega t - kz)] - y\}(S-h) \\ P_y = -\dfrac{c}{4\pi k}\times \\ \quad \times\{\cos[2(\omega t - kz)] + x\}(S-h) \end{cases} \tag{13}$$

It is seen that $P_x$, $P_x$ =0, when $S$=$h$. Thus, the averaged angular momentum is equal to zero in the vicinity of the $C$-point, when the vortex topological charge and the handedness factor have the same signs. In the opposite case ($S=-h$) one has

$$\begin{cases} P_x = -\dfrac{c}{4\pi k}2S\{S\sin[2(\omega t - kz)] - y\} \\ P_y = -\dfrac{c}{4\pi k}2S\{\cos[2(\omega t - kz)] + x\} \end{cases}. \tag{14}$$

Accordingly, the modules of the longitudinal and transversal components of the PV written in the coordinates $\rho, \varphi$ reduce to

$$\begin{cases} P_t = \dfrac{c}{2\pi k}\times \\ \quad \times\{1+\rho^2+2\rho\cos[2(\omega t - kz + S_C\varphi)]\}^{1/2}, \\ P_z = \dfrac{c}{4\pi}\times \\ \quad \times\{1+\rho^2+2\rho\cos[2(\omega t - kz + S_C\varphi)]\} \end{cases} \tag{15}$$

where $S_C$ is topological charge of the vibration phase at the $C$-point ($S_C = 1/2S$).

In this case, the transversal component module behaves similarly to the longitudinal one. It rotates with time around the $C$-point with the doubled oscillation frequency. The rotation direction of the minimum (or the maximum) is determined by the sign of topological charge of the vibration phase. The minimum $|P_z| = 0$ is reached on the $s$-contour and it corresponds to the position of the Nye's disclination [3,9-11]. For the specified distribution of complex amplitudes, the $s$-contour represents a circle centred at the $C$-point. Fig. 3 illustrates the temporal behaviour of the transversal component module. One can therefore expect that *the angular momentum similar to that observed in the vortex vicinity is observed in the $C$-point area.*

According to [21], $z$ component of the angular momentum density is given by the relation

$$j_z = xP_y - yP_x. \tag{16}$$

On the basis of Eqs. (15) and (16), the averaged angular momentum becomes

$$\overline{M} = -\frac{2S_C c^2}{\omega}J, \tag{17}$$

where $J = \int_0^{\rho_0}\rho^2 d\rho$ is defined by the "power" of the vortex beam in the actual area of cell with the diameter $2\rho_0$. Hence, the averaged angular momentum appears in the $C$-point vicinity when the signs of the topological charge of the vortex and the handedness factor are opposite and it equals to zero when those signs are the same.

## 4. Experimental investigation of the orbital angular momentum of $C$-point

It is obvious that the two following conditions must be fulfilled in order to prove experimentally the results of the theoretical analysis given above:

1. Formation of polarization-inhomogeneous field with easily controlled parameters is necessary. Naturally, the most convenient field is a field with only one $C$-point. The coordinates of the $C$-point should be easily determined and its topological charge must be easily changeable, depending on the experimental conditions. Certainly, the rotation direction of the field vector (i.e., the right-handed or left-handed polarization) in the $C$-point area has to be controlled, too.

2. It is necessary to have an "indicator" of presence of orbital angular momentum in the field.

As for the first condition, the polarization cell with the $s$-contour and $C$-point may be

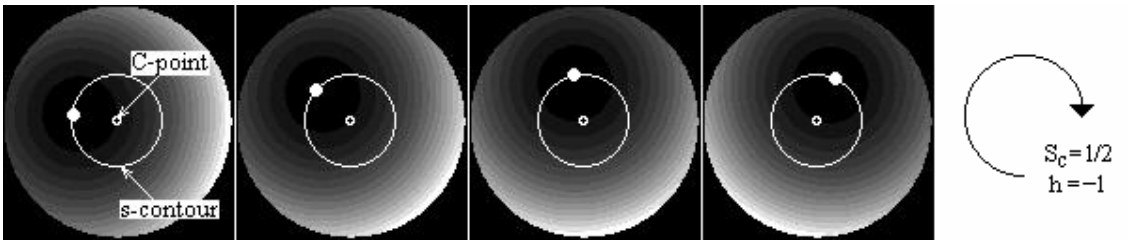


**Fig. 3.** Temporal behaviour of the module of transversal component around the $C$-point. White point corresponds to the energy density minimum. It is positioned on the $s$-contour and coincides with the Nye's disclination.

realized (as we have already mentioned above) as a superposition of two coaxially propagating, orthogonal circularly polarized beams. One of them is a circularly polarized isotropic vortex and the second one is an orthogonally polarized Gaussian beam. The $C$-point is localized in the vortex centre and the $s$-contour is formed along the line where the intensities of superposing beams are the same. Qualitative behaviour of polarization characteristics of such the field obtained by computer simulation is presented in Fig. 4. The rotation direction of the field vector (the left- or right-handed polarization) in the area bounded by the $s$-contour coincides with the corresponding direction in the Gaussian beam. Such the handedness factor is being changed to the opposite one while crossing the $s$-contour.

The sign of the orbital angular momentum arising in the $C$-point area, which is determined by the sign of topological charge of the vibration phase (see Eq. (17)), coincides with the "sign" of circularly polarized vortex. Notice that forming of the vortex with a necessary type of topological charge is not so a complex task. This may be performed easily enough with the vortex-generating hologram [37,38]. So, it is known that two single vortices with different signs are observed after the hologram, which correspond to diffraction orders $+1$ and $-1$ .

The resulting field may be obtained using interferometric techniques, for example, with the aid of Mach-Zehnder interferometer. Then the application of properly oriented $\lambda/4$ plates in different arms of the interferometer provides orthogonality of the superposing circularly polarized beams. Therefore, the first condition may be surely met.

As for the second one, unfortunately, the list of identification methods of the angular momentum is not so long [39]. In our opinion, in our experimental situation the most convenient is the method based on transferring angular momentum to some mechanical system. This technique for specifying orbital momentum is founded on the following points:

1 As it is known (see, e.g., [40]), an optical trap is being formed under focusing of laser beam. Such a trap can capture and hold micro-objects.

2. A rotation of micro-objects is observed if the field has a spin or orbital angular momentum (see [21-33]). The rotation frequency is governed by the magnitude of the momentum,

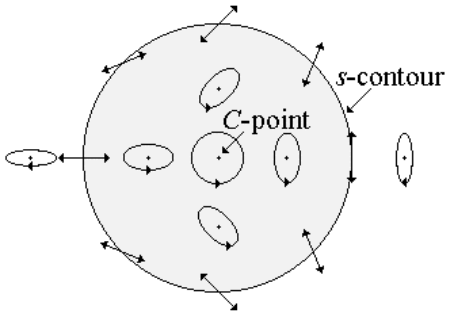


**Fig. 4.** Polarization cell obtained by superposition of circularly polarized vortex and orthogonally polarized Gaussian beam. Grey area corresponds to the field region with left-handed polarization. Topological charge $S_C$ of the *C*-point is equal to +1/2 and its sign coincides with that of topological charge of the vortex.

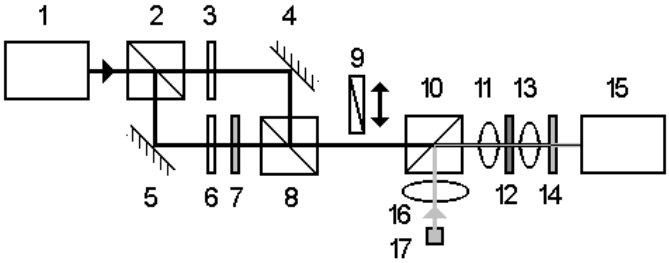


**Fig. 5.** Experimental setup for observing angular orbital momentum of polarization trap: 1 – He-Ne laser, 2,8 and 10 – beam splitters, 3 and 6 – $\lambda/4$ plates, 4 and 5 – mirrors, 7 – vortex-generating hologram, 9 – analyzer, 11 and 14 – micro-objectives, 12 – sample with particles, 14 – green filter, 12 – CCD camera, 16 and 17 – backlighting system.

while the rotation direction is specified by its sign.

3. In general, the focused beam has both the spin and orbital angular momenta. The rotation frequency is maximum when the signs of the momenta are the same and it becomes minimum (or even the rotation can change its direction) when those signs are opposite.

Thus, focusing of superposition of circularly polarized beams forms the optical trap, which is inhomogeneous in polarization. The micro-object captured by this trap rotates due to the angular momentum of the field. The rotation characteristics change with altering sign of topological charge of the circularly polarized vortex, because the sign of the orbital momentum also changes.

The experimental arrangement is presented in Fig 5. Linearly polarized beam of He-Ne laser is directed into Mach-Zehnder interferometer (see elements 2 to 8). It transforms into orthogonal circularly polarized beams due to $\lambda/4$ plates 3 and 6. Then one of the beams passes through vortex-generating hologram 7. The hologram reconstructs circularly polarized vortex. The field structure with the $s$-contour and $C$-point is formed at the output of interferometer.

Further, the resulting beam is focused with micro-objective 11 and then it is directed into the plane of sample with micro-particles 12. The result of effect of the beam on micro-particles is detected using the optical system 13 and 14, along with CCD camera. We have used a $60^x$ micro-objective with unit aperture with the purpose of forming the optical trap. The transversal size of the trap was 8 to 10 μm .

In order to determine polarization characteristics of the resulting field, we have chosen horizontal experimental arrangement. In this case, the acting beam passes through the optical surfaces without reflection. So, the polarization structure of the beam at the sample plane is the same as at the output of the interferometer. One can easily choose the sign (i.e., the direction of influence) of the orbital angular momentum while selecting the operating diffraction order of the vortex-generating hologram 7.

Fig. 6 illustrates the intensity distributions for the circularly polarized components of the resulting vector field. Analyzer 9 may be introduced into the beam for visualizing polarization modulation of the optical trap. The intensity distributions associated with different linear polarization projections corresponding to different orientations of analyzer 9 are presented in Fig. 7.

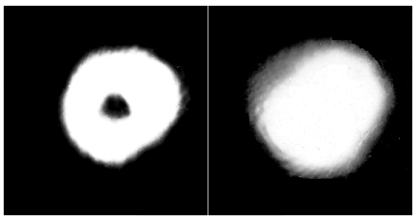

*a)* *b)*

**Fig. 6.** Intensity distributions for circularly polarized components of the trap field: (a) the vortex component and (b) the “smooth” beam.

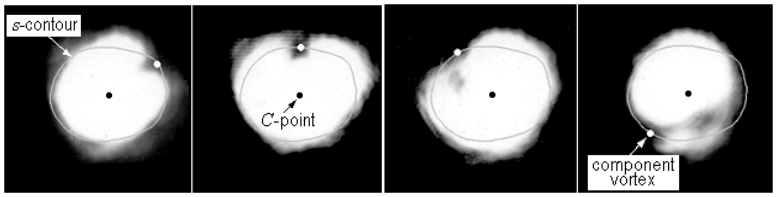


**Fig. 7.** Intensity distributions of different linear polarization projections of the trap field. The transmission axis of analyzer rotates in the counter-clockwise direction. Gray curve is experimentally specified $s$-contour. White point on the $s$-contour corresponds to the vortex projection position. The angular step for the analyzer axis orientation is approximately 30 deg.

The angular step linked to the transmission axis of analyzer equals approximately to 30 deg. The dark spot at the verge of the trap corresponds to the vortex component located on the *s*-contour. These points also indicate the positions of the minimum energy density (i.e., the Nye's disclination) [13], which goes along the $s$-contour with temporal changes of the vector field. As seen from Fig. 7, the intensities of the vortex beam and the "smooth" one are chosen in such a manner that the $s$-contour is located practically nearby the border of the trap. Due to this fact, the field has practically the same spin angular momentum sign throughout the trap. The coordinates of the $C$-point can be determined as those of the point inside the trap, which is characterized with the same intensity for all the polarization projections.

Thus, the field with the orbital momentum specified by the vortex and spin signs (without any changes in sign) is realized in the area of the trap with significant ("actual") intensity. It is this field region that influences the characteristics of rotation of micro-objects locked by the trap. Note that the spin momentum density decreases towards the $s$-contour, owing to decreasing ellipticity of polarization ellipses. Therefore, one can state that the area with efficient spin momentum adjoins directly the $C$-point and this area is significantly less than the dimension of the whole optical trap. Then the change in the sign of orbital momentum becomes apparent at the most for relatively large objects, whose dimensions are comparable with

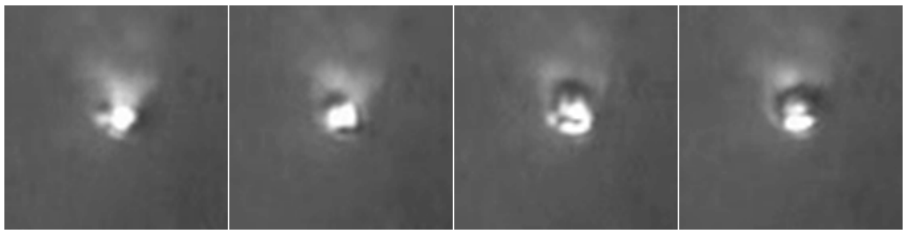


**Fig. 8.** Rotation of relatively large transparent particle due to the angular momentum (clockwise direction).

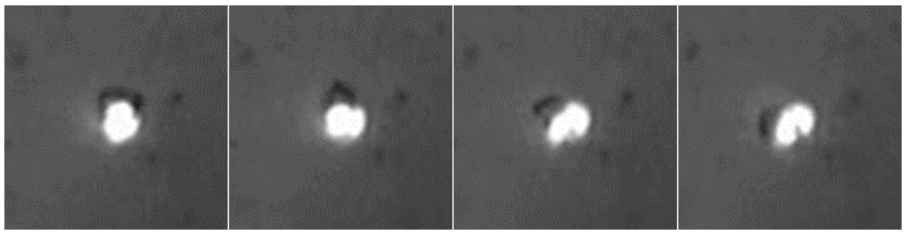


**Fig. 9.** Changes in the direction and speed of rotation of the captured particle due to changing sign of the orbital angular momentum.

those of the trap itself. Due to these reasons, the dimension of micro-particles (e.g., $Al_2O_3$ in oil) has been chosen to be comparable with the trap space. The behaviour of these relatively large captured particle is illustrated by Fig. 8 and 9.

It can be seen from Fig. 8 that the locked particle rotates in the clockwise direction. The rotation period is about 4–5 s. Fig. 9 corresponds to situation when the sign of the vortex beam is altered to the opposite, i.e. the orbital angular momentum changes its sign. The particle rotates in the opposite direction after such the operation and the rotation period is about 8–10 s. The difference in the rotation periods that takes place for the two above cases may be explained in the following way. In the former case, the spin momentum affects the particle in the same direction as the orbital momentum, while changing the topological charge of the *C*-point results in compensation of the orbital angular momentum by the spin one.

Another result of the influence of orbital angular momentum is illustrated in Fig. 10. Small dark absorbent particle is locked by a dark diffraction ring, which circumscribes the polarization trap. Unfortunately, only a part of the bright diffraction ring is seen in the figure, because the intensity in the trap centre is significantly higher than that of the diffraction ring. In addition, the intensity slightly changed along this ring. As a consequence, a small dynamical range of the CCD camera does not allow us to observe simultaneously the whole diffraction ring, the particle and the main area of the trap. However, it can be seen that, due to the orbital angular momentum, the particle rotates along the border of the "main" area of the trap in the clockwise direction. The dimension of the particle is about 2–4 $\mu m$. The revolution period is about 0.5 s.

## Discussion

As a result of our theoretical consideration and the experimental investigations, the appearance of orbital angular momentum in the vicinity of $C$-point is completely proved for the case when the topological vortex charge and the handedness factor have the opposite signs.

We have already noticed that the "importance" of optical singularities (including the polarization ones) as some junctions that "form" the structure of optical field is beyond question (see, e.g., [1,3-8,12-19]). At the same time, all the known facts associated with the subject of singular optics (except for optical tweezers based on the vortex beams) are not related to a *direct* influence of singular field structures on another physical system. In other words, all the achievements of singular optics are connected, in one way or another, with topological aspects of the formation of field structure. In particular, this yields the following consequence: *all the known methods*, which can *unambiguously* specify optical singularities, are indirect. For example, in order to determine the vortex, a reference beam is necessary, etc.

In this sense, arising of the orbital angular momentum in some area with the optical singularity conforms evidently to "physical" exclusiveness of the latter structures. Indeed,

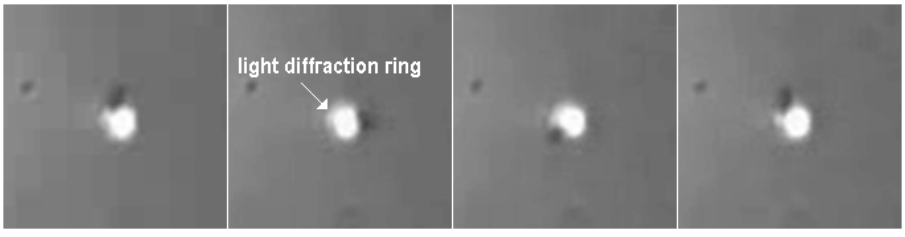


**Fig. 10.** Rotation of small dark absorbent particle captured by dark diffraction ring encircling the polarization trap (clockwise direction). The brightest of the light diffraction rings is depicted by a white arrow in figure (b).

due to that property of the field, some physical object placed in the field suffers specific *direct* influence.

In conclusion, we stress that the results of this paper concerned with the orbital angular momentum in the $C$-point vicinity have not only fundamental importance. In our opinion, they draw some applied interest. Namely, the principles of forming polarization-inhomogeneous optical trap may be used while elaborating *light* optical traps with controlled orbital angular momentum.

## Conclusions

Summing up the results of the present studies, we can state the following:

1. Physical manifestation of any optical singularity is, in one way or another, connected with a specific temporal behaviour of the field, no matter scalar or vector cases are realized. It becomes apparent when the angular momentum of the field of certain kind arises or disappears.

2. The orbital angular momentum is observed in the area of the $C$-point when the topological vortex charge and the handedness factor have the opposite signs. The direction of influence of this orbital angular momentum is defined by the sign of topological charge of the vibration phase in this area.

## References


1. Nye J.F. and Berry M. Proc. R. Soc. Lond. **A 336** (1974) 165.
2. Baranova N.B., Mamayev A.V., Pilipetsky N.F., Shkunov V.V., Zeldovich B.Ya. J. Opt. Soc. Am. **A 73** (1983) 525.
3. Nye J.F. Natural focusing and fine structure of light, Institute of Physics Publishing, Bristol and Philadelphia, (1999).
4. Nye J.F., Hajnal J.V. and Hannay J.H. Proc. R. Soc. Lond. **A 417** (1988) 7.
5. Freund I.and Shvartsman N. Phys. Rev. A **50** (1994) 5164.
6. Freund I., Shvartsman N. and Freilikher V. Opt. Commun. **101** (1993) 247.
7. Freund I. Proc. SPIE **2389** (1995) 411.
8. Mokhun I. Proc.SPIE **3573** (1998) 567.
9. Nye J.F. Proc. R. Soc. Lond. **A 387** (1983)105.
10. Nye J.F. Proc. R. Soc. Lond. **A 389** (1983) 279.
11. Nye J.F. and Hajnal J.V. Proc. R. Soc. Lond. **A 409** (1987) 21.
12. Hajnal J.V. Proc. R. Soc. Lond. **A 414** (1987) 433.
13. Angelsky O., Besaha R., Mokhun A., Mokhun I., Sopin M., Soskin M., Vasnetsov M. Proc. SPIE **3904** (1999) 40.
14. Angelsky O., Mokhun A., Mokhun I. and Soskin M. Opt. Commun. **207** (2002) 57.
15. Angelsky O., Besaha R., Mokhun I., Sopin M., Soskin M. Proc. Chernivtsy University, Ser. Physics, Ed. O. Angelsky **57** (1999) 88.
16. Freund I., Soskin M. and Mokhun A., Opt. Commun. **208** (2002) 223.
17. Angelsky O., Mokhun A., Mokhun I. and. Soskin M, Phys. Rev. E. **65** (2002) 036602.
18. Freund I. Opt. Commun. **199** (2001) 47.
19. Freund I. Opt. Commun. **201** (2002) 251.
20. Berry M. and Dennis M. Proc. R. Soc. Lond. **A 457** (2001) 141.
21. Allen L., Padgett M.J. and Babiker M., The orbital angular momentum of light E. Wolf, Progress in optics XXXIX, Elsevier Science B.V. (1999).
22. Berry M. Proc. SPIE **3487** 6 (1998).
23. Allen L., Beijesbergen M.W., Spreeuw R.J.C. and Woerd-man J.P., Phys. Rev. A **45** (1992) 8185.
24. He H., Friese M.E.J., Heckenberg N.R. and Rubinsztein -Dunlop H. Phys. Rev. Lett. **75** (1995) 826.
25. Friese M.E.J., Niemenen T.A., Heckenberg N.R. and Rubinsztein-Dunlop H., Nature (London) **394** (1998)348.
26. Simpson N.B., Dholakia K., Allen L.and Padgett M. Opt. Lett. **22** (1997) 52.
27. Volke-Sepulveda K.,Garcés-Chávez V., Chá-vez-Cerda S., Arlt J. and Dholakia K. J. Opt. B: Quantum Semiclassical Opt.**4** (2002) 582.

28. O'Neil A.T. and Padgett M.J. Opt. Commun. **184** (2000) 139.
29. O'Neil A.T., McVicar I., Allen L. and Padgett M.J. Phys. Rev. Lett. **88** (2001) 053601.
30. Allen L. and Padgett M.J. Opt. Commun. **184** (2000) 67.
31. Arlt J. and Dholakia K. Opt. Commun. **177** (2000) 297.
32. Garce´s-Cha´vez V., Volke-Sepulveda K., Chávez-Cerda S., Sibbett W. and Dholakia K. Phys. Rev. A **66** (2002) 063402.
33. Garce´s-Cha´vez V., McGloin D., Padgett M. J., Dultz W., Schmitzer H. and Dholakia K. Phys. Rev. Lett. **91** (2003) 093602.
34. Mokhun I., Arkhelyuk A., Brandel R. and Viktorovskaya Ju.Proc. SPIE **5477**(2004) 47.
35. Mokhun I., Mokhun A., Viktorovskaya Ju., Cojoc D., Angelsky O. and Di Fabrizio E. Proc. SPIE **5514** (2004) 652.
36. Berry M.V., Jeffery M.R. and Mansuripor M. J. Opt. A: Pure Appl. Opt. **7** (2005) 685.
37. White A.G., Smith C.P., Heckenberg N.R., Rubinsztein-Dunlop H., McDuff R. , Weiss C.O. and Tamm Chr. J. Mod. Opt. **38** (1991) 2531.
38. Bazhenov V.Yu., Vasnetsov M.V. and Soskin M. S. Sov. Phys. JETP Lett. **52** (1990). 429.
39. Leach J., Padgett M.J., Barnett S.M., Franke-Arnold S. and Courtial J. Phys. Rev. Lett. **88** (2002) 257901-1.
40. Ashkin A., Dziedzic J.M., Bjorkholm J.E. and Chu S. Opt. Lett. **11** (1986) 288.